

Tetrahydropentalenyl-phosphazene constrained
geometry complexes of rare-earth metal alkyls†Cite this: *Dalton Trans.*, 2014, **43**,
7109Noa K. Hangaly, Alexander R. Petrov, Michael Elfferding, Klaus Harms and
Jörg Sundermeyer*

Reactions of $\text{Cp}^{\text{TM}}\text{HPPH}_2$ (**1**, diphenyl(4,4,6,6-tetramethyl-1,4,5,6-tetrahydropentalen-2-yl)phosphane) with the organic azides AdN_3 and DipN_3 (Ad = 1-adamantyl; Dip = 2,6-di-iso-propylphenyl) led to the formation of two novel CpPN ligands: *P*-amino-cyclopentadienyldiene-phosphorane ($\text{Cp}^{\text{TM}}\text{PPh}_2\text{NHAd}$; **L_{Ad}H**) and *P*-cyclopentadienyl-iminophosphorane ($\text{Cp}^{\text{TM}}\text{HPPH}_2\text{NDip}$; **L_{Dip}H**). Both were characterized by NMR spectroscopy and X-ray structure analysis. For both compounds only one isomer was observed. Neither possesses any detectable prototropic or elementotropic isomers. Reactions of these ligands with $[\text{Lu}(\text{CH}_2\text{SiMe}_3)_3(\text{thf})_2]$ or with rare-earth metal halides and three equivalents of $\text{LiCH}_2\text{SiMe}_3$ produced the desired bis(alkyl) $\text{Cp}^{\text{TM}}\text{PN}$ complexes: $[(\text{Cp}^{\text{TM}}\text{PN})\text{M}(\text{CH}_2\text{SiMe}_3)_2]$ (M = Sc (**1_{Ad}**, **1_{Dip}**), Lu (**2_{Ad}**, **2_{Dip}**), Y (**3_{Ad}**, **3_{Dip}**), Sm (**4_{Ad}**), Nd (**5_{Ad}**), Pr (**6_{Ad}**), Yb (**7_{Ad}**)). These complexes were characterized by extensive NMR studies for the diamagnetic and the paramagnetic complexes with full signal assignment. An almost mirror inverted order of the paramagnetic shifts has been observed for ytterbium complex **7_{Ad}** compared to **4_{Ad}**, **5_{Ad}** and **6_{Ad}**. For the assignment of the NMR signals $[(\eta^1:\eta^5\text{-C}_5\text{Me}_4\text{PMe}_2\text{NAd})\text{Yb}(\text{CH}_2\text{SiMe}_3)_2]$ **7** was synthesized, characterized and the ^1H NMR signals were compared to **7_{Ad}** and to other paramagnetic lanthanide complexes with the same ligand. **1_{Ad}**, **2_{Ad}**, **2_{Dip}**, **3_{Ad}** and **3_{Dip}** were characterized by X-ray structure analysis revealing a sterically congested constrained geometry structure.

Received 21st December 2013,
Accepted 20th February 2014

DOI: 10.1039/c3dt53596g

www.rsc.org/dalton

Introduction

The organometallic chemistry of the rare-earth metals began in the middle of the last century with the synthesis of their tris-(cyclopentadienyl) derivatives by Wilkinson and Birmingham.¹ Since then the cyclopentadienyl (Cp) ligand has remained one of the most ubiquitous ligands of this chemistry. For a long time, rare-earth organometallic chemistry has been dominated by metallocenes,² especially when these complexes are used as precursors in various stoichiometric and catalytic processes.³ More recently, however, considerable attention has been directed towards rare-earth *mono*-cyclopentadienyl complexes.⁴ But the selective synthesis of monomeric rare-earth metal *mono*-Cp complexes is generally difficult. A great steric bulk of the Cp ligand is advantageous for a successful synthesis. In search of better ligand systems, wide variations of the aromatic

cyclopentadienyl framework have been described in the literature.^{4,5} These variations include for example totally or partly substituted Cp rings and ancillary linked donor atoms like O, N, P or S. The latter are used to form constrained geometry complexes (CGCs).⁶

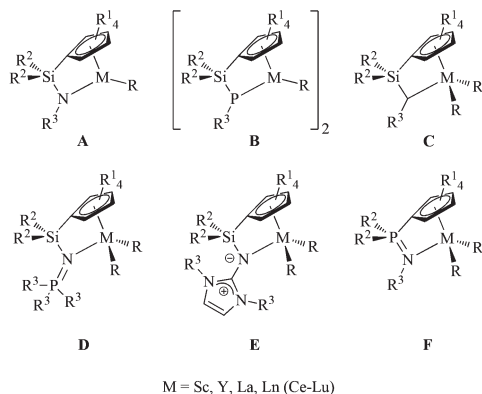
In this work we describe the synthesis, NMR studies and molecular structures of two novel cyclopentadienyl-phosphazene (CpPN) ligands with a tetrahydropentalene unit: $\text{Cp}^{\text{TM}}\text{PPh}_2\text{NHAd}$ (**L_{Ad}H**) and $\text{Cp}^{\text{TM}}\text{HPPH}_2\text{NDip}$ (**L_{Dip}H**). This tetrahydropentalene unit is very attractive as it is easily synthesized by condensation of NaCp with Ph_2PCl and two equivalents of acetone. Compared to other sterically demanding cyclopentadienyls such as $\text{C}_5\text{Me}_4\text{R}$, it is cheap and can easily be synthesized on a large scale. The new ligands bear a sterically very demanding, well crystallizing, electron rich and rigid cyclopentadienyl ring. Therefore we are confident that these and related tetrahydropentalenyl ligands are good alternatives for the commonly used but expensive $\text{C}_5\text{Me}_4\text{R}$ building blocks in organometallic chemistry.

Constrained geometry complexes with the cyclopentadienyl-silylamido (CpSiN) type ligands, initially developed by Bercaw^{7–9} and Okuda,¹⁰ became one of the best developed classes of CGCs (Scheme 1; **A**). In contrast, however, constrained geometry rare-earth metal(III) complexes with different single-atom bridging units in the ligand system have received

Fachbereich Chemie der Philipps-Universität Marburg, Hans-Meerwein-Straße,
35032 Marburg, Germany. E-mail: jsu@staff.uni-marburg.de;

Fax: +49 6421 2825711; Tel: +49 6421 2825693

†Electronic supplementary information (ESI) available: Experimental details for X-ray crystallographic studies, detailed NMR experiments (^1H , ^{31}P , ^{13}C and 2D NMR experiments) with signal assignment and crystallographic information files (CIF). CCDC 817338–817344. For ESI and crystallographic data in CIF or other electronic format see DOI: 10.1039/c3dt53596g



Scheme 1 Examples of known constrained geometry rare-earth metal complexes.

much less attention and have remained almost unexplored to date. Some examples are CpSiP complexes (**B**)¹¹ and CpSiC complexes (**C**)¹² which have dianionic ligands. There are also some complexes bearing monoanionic ligands which are iso-electronically related to the classical dianionic CpSiN ligand system such as CpSiNP (**D**),¹³ CpSiNim (**E**)¹⁴ and the cyclopentadienyl-phosphazenes (CpPN) (**F**) that is the focus of our current investigation.^{15–19}

Previously we reported a general and convenient synthetic protocol for a large variety of CpPN type ligands,²⁰ and their use in the stabilization of highly reactive alkyls of rare-earth and group 4 metals has been claimed.²¹ Independently, related fluorenyl- and indenyl-phosphazene ligands (FluPN and IndPN) and their rhodium²² and zirconium²³ complexes were presented by Bourissou and co-workers. The synthesis and characterization of a series of rare-earth metal constrained geometry CpPN complexes [$\{\eta^5, \eta^1\text{-C}_5\text{Me}_4\text{PMe}_2\text{NAd}\}\text{-M}(\text{CH}_2\text{SiMe}_3)_2$] (M = Sc, Lu, Y, Sm, Nd, Pr, Ce) and their high catalytic activities in the intramolecular hydroamination/cyclization have been reported by us.^{15,17} Recently, the organometallic chemistry and catalysis in ethylene polymerization of rare-earth metal CpPN, IndPN and FluPN complexes was studied. CpPN ligands, with less steric bulkiness of the Cp-ring, lead to the coordination of THF, while IndPN adopt a η^3 -bonding fashion and the more bulky FluPN-type ligands display a η^1 -bonding mode.¹⁸ Moreover, the reactivity toward various substrates was recently studied and, among others, CpPN amidinate, hydride and terminal imido complexes were synthesized, characterized and their reactivity was probed.¹⁹

These current developments reveal that CpPN type complexes appear to be a promising class of catalysts. Therefore it is of general and fundamental interest to develop novel, sterically most demanding and rigid CpPN type ligands as useful building blocks and to study their stabilizing properties for dialkyls of the smallest and larger rare-earth metal cations (Sc, Lu, Y, Yb, Sm, Nd and Pr). Besides synthetic and XRD structural aspects, the focus of this study will be on the beautiful ¹H and ¹³C NMR spectra obtained from paramagnetic organometallic compounds carrying the chelating rigid

CpTMPPh₂NHAd (**L_{Ad}H**) and CpTMHPPh₂NDip (**L_{Dip}H**) ligands with the tetrahydropentalene unit. Assignment of ligand group shifts of paramagnetic organometallic lanthanide complexes is not routinely reported in literature, but it might become a very valuable tool for following catalytic steps.

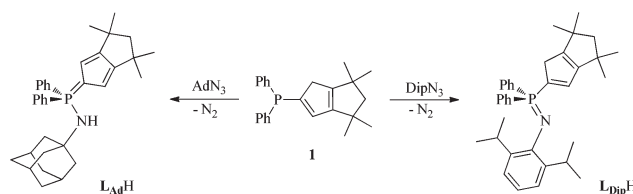
Results and discussion

Synthesis and characterization of the CpTMPN-ligands

The ligands were prepared by a Staudinger reaction (Scheme 2) of the novel phosphane CpTMHPPh₂ (**1**, diphenyl(4,4,6,6-tetramethyl-1,4,5,6-tetrahydropentalen-2-yl)phosphane)²⁴ with organic azides (AdN₃ and DipN₃; Dip = 2,6-di-iso-propylphenyl). It should be mentioned that compared to our previously published synthesis of **1** we could exchange the highly toxic TlCp by NaCp, which can easily be synthesized on a large scale out of Na and (CpH)₂.²⁵ The improved ligand synthesis is following the condensation of NaCp with one Ph₂PCl and two acetone molecules, which are cheap starting materials making the final CpTMPN ligand very attractive as an alternative for commonly used but expensive ligands with a C₅Me₄R moiety.

The Staudinger reaction of the highly crowded CpTMHPPh₂ **1** with AdN₃ proceeds very slowly. Therefore, under classical Staudinger conditions a reaction time of 10 d is needed in refluxing THF, yielding **L_{Ad}H** (CpTMPPh₂NHAd) in only 46% yield. Higher reaction temperatures accelerate the reaction and it was completed after only 2 d in refluxing toluene. The yellow crystalline compound **L_{Ad}H** was isolated from *n*-hexane in 75% yield. In contrast, the oxidation with the more electron-poor DipN₃ was completed within 14 h in THF at room temperature. The desired, sterically demanding ligand **L_{Dip}H** (CpTMHPPh₂NDip) was obtained in 78% yield after crystallization from cold acetonitrile.

Compared to **L_{Dip}H**, which is a highly air-sensitive substance with a melting point of 142.4–143.0 °C and a high solubility in *n*-hexane, compound **L_{Ad}H** is only moderately air-sensitive, has a higher melting point (176.5–177.0 °C) and is only marginally soluble in *n*-hexane. Further investigations by means of NMR spectroscopy and X-ray structure analysis show significant dissimilarities in their molecular compositions: compound **L_{Ad}H** occurs in the form of *P*-amino-cyclopentadienyl-phosphorane, whereas **L_{Dip}H** exists in the tautomeric form of a *P*-cyclopentadienyl-imino-phosphorane.



Scheme 2 Synthesis of the ligands **L_{Ad}H** and **L_{Dip}H** by Staudinger reaction.



NMR spectroscopy

The ^{31}P NMR signal of L_{AdH} (15.6 ppm) is essentially identical to those of compound $\text{C}_5\text{Me}_4\text{PR}_2\text{NHAd}$ (17.6 for $\text{R} = \text{Me}^{15}$ and 12.3 ppm for the main isomer in $\text{R} = \text{Ph}^{16}$ resp.). In contrast, compound L_{DipH} shows a ^{31}P NMR resonance at -15.8 ppm. This chemical shift is in good agreement with the iminophosphorane tautomer $\text{IndPPh}_2=\text{NR}$ ($\text{Ind} = \text{indenyl-1}$; $\delta_{\text{P}} = -8.3$ and -16.5 ppm for $\text{R} = \text{Ph}$ and Dip resp.).²³ However, in contrast to $\text{C}_5\text{Me}_4\text{PPh}_2\text{NHAd}$,¹⁶ $\text{C}_5\text{Me}_4\text{HPMe}_2\text{NR}$ ($\text{R} = \text{SiMe}_3$, Dip)²⁰ and $\text{IndPPh}_2=\text{NR}$ ($\text{R} = \text{Ph}$ and Dip),²³ L_{AdH} and L_{DipH} show only one sharp resonance in the ^{31}P NMR spectra, indicating the absence of isomers. Recently, we also observed only one tautomer in $\text{C}_5\text{Me}_4\text{HPR}_2\text{NC}_6\text{H}_3\text{R}'_2$ ($\text{R} = \text{Me}$, $\text{R}' = \text{iPr}$; $\text{R} = \text{Ph}$, $\text{R}' = \text{Me}$, iPr) at thermodynamic equilibrium.¹⁸

The resonance of the NH-proton in L_{AdH} at $\delta_{\text{H}} = 2.05$ ppm appears as a doublet ($^2J_{\text{HP}} = 5.0$ Hz). It does not correlate with any carbon atom in the molecule according to the HMQC correlation spectrum. This confirms the presence of an amino-phosphorane. Unlike L_{AdH} , compound L_{DipH} shows four resonances in the aliphatic region (besides resonances of isopropyl (Dip) protons) which resemble the pattern of the parent phosphane **1**. Especially the allylic CH_2 group at $\delta_{\text{H}} = 3.08$ ppm confirms that the ligand is in the imino-phosphorane form in solution (for spectra see ESI†). No tautomerization or isomerization could be observed for L_{AdH} and L_{DipH} by multinuclear NMR spectroscopy in C_6D_6 .

X-Ray structure analysis

The compound L_{AdH} crystallizes from benzene at room temperature with two disordered solvent molecules per unit cell. Compound L_{DipH} crystallizes without incorporated solvent molecules. Both compounds crystallize in monoclinic crystal systems (space groups $P2_1/n$ and $P2_1/c$ resp.) with 4 units in the unit cell (Fig. 1). Selected bond lengths (\AA) and angles ($^\circ$) for L_{AdH} and L_{DipH} are presented in Table 1. In the structure of compound L_{DipH} one of the iso-propyl groups is disordered and treated with an occupancy factor of 63 : 37.

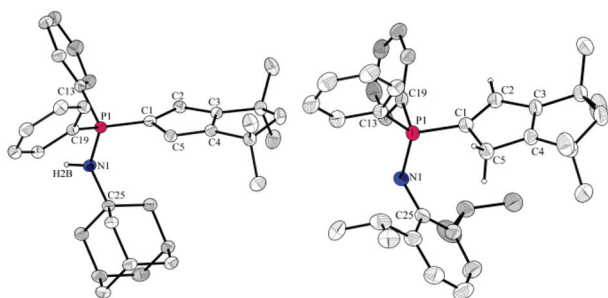


Fig. 1 Molecular structures of $\text{L}_{\text{AdH}} \times 2\text{C}_6\text{H}_6$ and L_{DipH} . All hydrogen atoms, except N–H for L_{AdH} and protons of the C5-ring for L_{DipH} , have been omitted for clarity. Incorporated benzene molecules and disordered iso-Pr group with lower occupancies have also been omitted for clarity.

Table 1 Selected bond lengths (\AA) and angles ($^\circ$) for L_{AdH} and L_{DipH}

	L_{AdH}	L_{DipH}
P1–N1	1.652(2)	1.556(2)
P1–C1	1.704(2)	1.788(2)
P1–C13	1.799(2)	1.819(2)
P1–C19	1.801(2)	1.806(2)
N1–C25	1.494(3)	1.408(2)
C1–P1–N1	115.6(1)	115.2(1)
C13–P1–N1	102.6(1)	113.2(1)
C19–P1–N1	110.0(1)	110.1(1)
C1–P1–C13	112.5(1)	106.6(1)
C13–P1–C19	106.4(1)	103.0(1)
C19–P1–C1	109.3(1)	108.0(1)
C1–P1–N1–C25	37.5(2)	17.5(2)

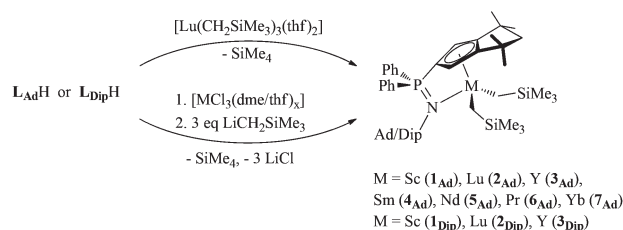
The cyclopentadienyl rings of both ligands are essentially planar; the largest deviations from the ideal C5 plane are $\Delta_{\text{max}} = 0.004(2)$ for L_{AdH} and $0.006(2)$ \AA for L_{DipH} resp.

As anticipated the P–C_{Cp} bond length in P-ylide L_{AdH} is quite short, P1–C1 1.704(2) \AA , and can be compared with $d(\text{P–C}_{\text{Cp}})$ 1.718(2) \AA in $\text{Ph}_3\text{P}=\text{C}_5\text{H}_4$ ²⁶ while the P–N bond length 1.652(2) \AA is rather long. This can be better compared with the values found in phosphonium salts $[\text{Ph}_3\text{P–NH}(\text{iso-Pr})]^+\text{Br}^-$ (P–N = 1.621(3) \AA).²⁷ The C–C bonds of the Cp ring of L_{AdH} are conjugated (average bond length $d(\text{C–C}) = 1.41$ \AA , maximum C–C bond difference $d = 0.07$ \AA). The parameters resemble the expected values for a cyclopentadienyldene-aminophosphorane structure.

The structure of L_{DipH} is unexceptional with a short P–N bond length of 1.556(2) \AA , typical for imino-phosphoranes (compare: $\text{Ph}_3\text{P}=\text{N}(2,6\text{-C}_6\text{H}_3)$ (1.553(2) \AA)²⁸ and $\text{Ph}_3\text{P}=\text{N}(\text{tert-Bu})$ (1.543(2) \AA)).²⁶ The alternating bond order and the bond lengths in the CpTM-moiety are similar to those found in the parent phosphine CpTMHPPh₂ **1**²⁴ and lie in ranges typical for cyclopentadiene compounds.²⁹ The P1–C1 1.788(2) \AA is significantly larger than that in L_{AdH} . Moreover, this value is much closer to P–C_{Ph} bond lengths where a C(sp²)–P bond is present.

Preparation and characterization of CpTMPN rare-earth metal alkyls

For the syntheses of the lutetium complexes, $[\text{Lu}(\text{CH}_2\text{SiMe}_3)_3(\text{thf})_2]$ was used and the complexes were isolated in high yields as microcrystalline, colourless solids $[\{\text{L}_{\text{Ad}}\}\text{Lu}(\text{CH}_2\text{SiMe}_3)_2]$ (**2Ad**) and $[\{\text{L}_{\text{Dip}}\}\text{Lu}(\text{CH}_2\text{SiMe}_3)_2]$ (**2Dip**) (Scheme 3). For the



Scheme 3 Synthesis of complexes $[\{\text{Cp}^{\text{TM}}\text{PN}\}\text{M}(\text{CH}_2\text{SiMe}_3)_2]$.



other rare-earth metals (Sc, Y, Sm, Nd, Pr and Yb), the complexes were synthesized under essentially the same reaction conditions reported for $[(C_5Me_4PMe_2NAd)M(CH_2SiMe_3)_2]$ complexes.^{15,17} Following this *in situ* protocol three equivalents of $LiCH_2SiMe_3$ were added to a stirred suspension of an equimolar mixture of the respective $\{Cp^{TMPN}\}H$ ligand ($L_{Ad}H$, $L_{Dip}H$) and a rare-earth metal halide source in ether–toluene or ether–*n*-hexane at 0 °C. Filtration, solvent removal, extraction with *n*-hexane and crystallization afforded the Cp^{TMPN} complexes $[(L_{Ad})M(CH_2SiMe_3)_2]$ ($M = Sc$ (**1_{Ad}**), Y (**3_{Ad}**), Sm (**4_{Ad}**), Nd (**5_{Ad}**), Pr (**6_{Ad}**), Yb (**7_{Ad}**)) and $[(L_{Dip})M(CH_2SiMe_3)_2]$ ($M = Sc$ (**1_{Dip}**), Y (**3_{Dip}**)) (Scheme 3).

The complexes **1_{Ad}**–**7_{Ad}**, and **1_{Dip}**–**3_{Dip}** are fairly air- and moisture-sensitive solids and show good solubility in saturated hydrocarbons and high solubility in ethers and aromatic solvents. All complexes were fully characterized by NMR spectroscopy and elemental analysis, and complexes **1_{Ad}**, **2_{Ad}**, **3_{Ad}**, **2_{Dip}** and **3_{Dip}** were also characterized by X-ray structure analysis.

The complexes with ligand L_{Dip} reveal a different thermostability in comparison with those bearing ligand L_{Ad} . Compounds **1_{Dip}**–**3_{Dip}** appear to be less stable than the analogue complexes **1_{Ad}**–**3_{Ad}**. Complexes **1_{Dip}** and **2_{Dip}** are still stable at room temperature in solution but decompose fast at elevated temperatures. Yttrium complex **3_{Dip}** is not stable at room temperature both in solution and in the solid state. Thus, for larger metals such as samarium, no stable complex could be isolated with this ligand.

Multinuclear NMR spectroscopy of CpPN complexes

All complexes were established by NMR spectroscopy. The ^{31}P NMR spectra of diamagnetic **1_{Ad}**–**3_{Ad}** and **1_{Dip}**–**3_{Dip}** complexes appear in the region 6.4–7.3 and 8.9–9.3 ppm, respectively. The ^{31}P resonances of the paramagnetic complexes **4_{Ad}**–**7_{Ad}** are broadened signals at $\delta = 24.4$ (**4_{Ad}**, $M = Sm$), -92.00 (**5_{Ad}**, $M = Nd$), -66.0 (**6_{Ad}**, $M = Pr$) and -117.2 (**7_{Ad}**, $M = Yb$).

According to the 1H and ^{13}C NMR spectroscopy, **1_{Ad}**–**7_{Ad}** and **1_{Dip}**–**3_{Dip}** crystallize without coordinated solvent molecules, whereas complexes with less steric bulkiness of the Cp-ring in $[(C_5H_4PPh_2NDip)M(CH_2SiMe_3)_2(thf)]$ ($M = Lu, Y, Sm,$

Nd) are isolated with a coordinated THF molecule.¹⁸ 1H NMR spectra of the diamagnetic **1_{Ad}**–**3_{Ad}** and **1_{Dip}**–**3_{Dip}** complexes are very similar (for spectra see ESI†); therefore only some main aspects should be discussed here. Because of the η^5 -coordination of the Cp ring, Cp protons appear as one doublet at about 6.2 ppm with a $^3J_{HP}$ of about 3 Hz. The signals of the methyl and methylene group in the annulated five membered ring are, because of their fixed *exo*- and *endo*-positions, chemically inequivalent. Consequently, the methyl group resonances appear as two singlets and the resonances of the methylene group appear as two doublets ($^2J_{HH}$ about 12 Hz). Silylmethylene protons are, like in $[(C_5Me_4PMe_2NAd)M(CH_2SiMe_3)_2]$,¹⁷ diastereotopic and for that magnetically non-equivalent. They appear as two doublets in all spectra. For yttrium complexes the protons appear as two doublet of doublets due to Y–H-coupling ($^2J_{HH} = 11.2$ Hz, $^2J_{HY} = 2.7$ Hz). Furthermore, in this case the methylene carbons show a doublet with a $^1J_{CY}$ coupling of 40.9 Hz in the ^{13}C NMR spectrum. Both are in the same range as shown in the literature, for example for classic $[\eta^5-\eta^1-CpSiN]Y(CH_2SiMe_3)(thf)]$ CGC.³⁰

Lanthanides have a short relaxation time for the unpaired electron so that little line broadening occurs. The mechanism of action within the lanthanides is principally the pseudocontact mechanism, which falls off in a predictable manner with distance ($1/R^3$).³¹ The direction of shift depends on the anisotropy in the susceptibility, but it also depends on the angle between the principal axis of susceptibility and the vector *R* to the nucleus. Despite this principal insight, systematic NMR studies on paramagnetic organolanthanide compounds are not a routine characterization method.³² NMR studies are typically restricted to the diamagnetic derivatives ($Lu(III)$, Sc, Y, and $La(III)$),^{2,4} whereas some of the best catalysts are obtained with the paramagnetic metal cations like neodymium or samarium.^{3,4} Here we report 1H NMR spectra recorded in C_6D_6 at 27 °C of paramagnetic complexes **4_{Ad}**–**7_{Ad}** that show defined, relatively sharp signals with distinctive paramagnetic shifts, indicating a rigid constrained-geometry structure in solution. The assignment of the NMR signals for complexes **4_{Ad}**–**6_{Ad}** requires 2D NMR experiments due to the paramagnetic shift. The signals are summarized in Table 2. The width

Table 2 1H NMR resonances (δ /ppm) and coupling constants (J/Hz) of the paramagnetic complexes **4_{Ad}**–**7_{Ad}** in C_6D_6 at 27 °C

	4_{Ad} (f^5Sm^{3+})	5_{Ad} (f^3Nd^{3+})	6_{Ad} (f^2Pr^{3+})	7_{Ad} ($f^{13}Yb^{3+}$)
Ln-HCH	12.65, 12.52	33.48, 30.19	99.51, 93.03	–239.26, –225.45
CpH	10.87	12.03	30.03	–117.29
<i>o</i> -PhH	10.34	15.40	20.73	–28.92
<i>m</i> -PhH ($^3J_{HH}$)	7.94 (7.5)	9.92	12.08 (6.8)	–7.77
<i>p</i> -PhH ($^3J_{HH}$)	7.74 (7.4)	9.13	10.65 (6.8)	–3.77
SiMe ₃	1.70	4.30	6.08	–29.57
<i>exo</i> - δ -AdH ($^2J_{HH}$)	–0.56	–4.93 (10.2)	–10.72 (10.5)	38.85
γ -AdH	–0.73	–6.47	–14.21	51.24
<i>endo</i> - δ -AdH ($^2J_{HH}$)	–1.12 (11.6)	–7.52 (11.9)	–14.90 (10.5)	49.65
<i>exo</i> -MeCMe	–1.29	–5.48	–11.93	41.74
<i>endo</i> -MeCMe	–1.58	–13.41	–21.50	65.27
<i>exo</i> -HCH(CMe ₂) ₂ ($^2J_{HH}$)	–2.15 (12.7)	–12.29 (8.5)	–23.81 (10.0)	81.49
<i>endo</i> -HCH(CMe ₂) ₂ ($^2J_{HH}$)	–4.80 (12.7)	–24.05 (10.2)	–45.27 (10.0)	148.51
β -AdH	–7.18	–27.26	–52.96	162.74



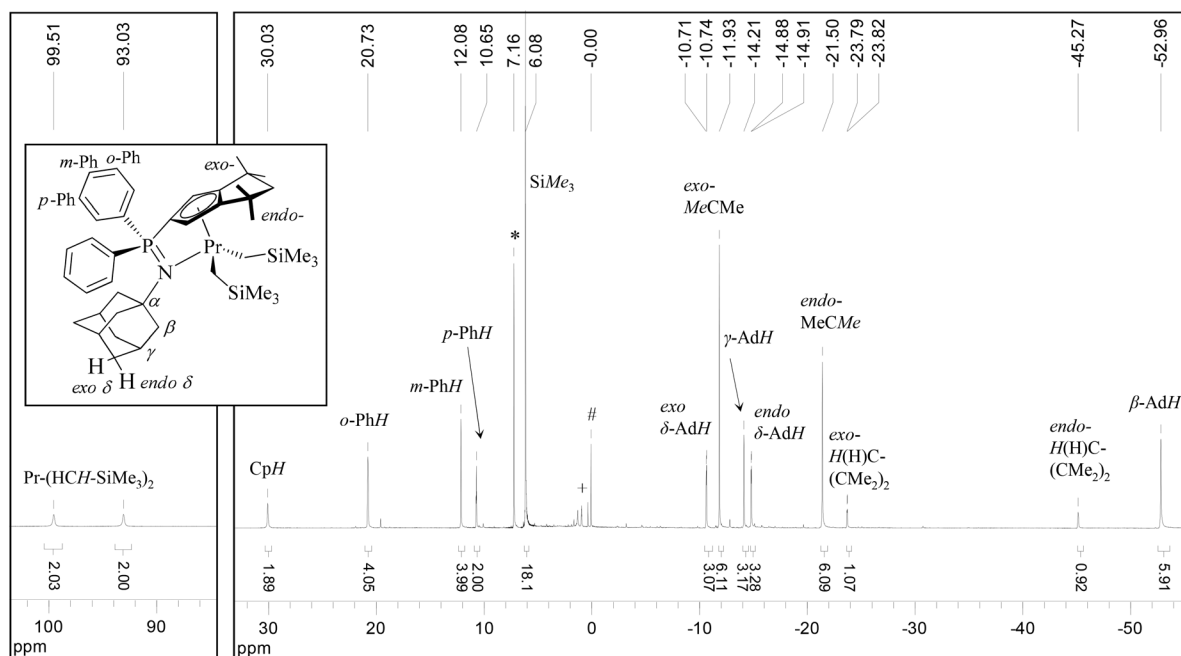


Fig. 2 Two sections out of the ^1H NMR spectrum (300.1 MHz) of complex $[(\text{L}_{\text{Ad}})\text{Pr}(\text{CH}_2\text{SiMe}_3)_2]$ (6_{Ad}) in C_6D_6 at 27°C . The resonances denoted with (#), (+) and (*) are assigned to SiMe_4 , silicon grease and the residual protons of C_6D_6 .

of the resonances at half-height ($\nu_{1/2}$) is shown in the Experimental section.

In Fig. 2, the NMR spectrum of $f^2\text{Pr}^{3+}$ complex 6_{Ad} which ranges from +100 to -53 ppm is shown as a representative example (for other spectra see ESI†).

All resonances of the adamantyl and annulated five-ring moiety protons are shifted upfield while the CH_2SiMe_3 alkyl groups, the phenyl substituents on the phosphorus and the cyclopentadienyl protons are shifted downfield.

Because of the paramagnetic shifting, the signals of the phenyl protons are distributed over a wide range. The $o\text{-PhH}$ are furthest downfield shifted due to the relatively small distance to the paramagnetic metal centre. The $m\text{-PhH}$ and $p\text{-PhH}$ resonances are less shifted as they are located further away from the metal centre. Using the dependence of the paramagnetic shift on the distance to the metal centre, one can specify the methylene and methyl group resonances of the annulated five ring moiety. The methylene and methyl group resonances that are more upfield shifted are the ones closer to the paramagnetic centre (*exo*-proton/group) leaving the other to be the *endo*-proton/group.

For the $\text{Sm}(\text{III})$ complex the ^{13}C NMR spectrum was showing similar but only slightly paramagnetically shifted signals compared to those of the diamagnetic homologues.

CpPN complexes of ytterbium(III) have never been described before. The ^1H NMR spectrum of $f^{13}\text{Yb}^{3+}$ complex 7_{Ad} reaches from -240 to $+163$ ppm but still shows all the expected defined signals. For unambiguous assignment of all the NMR signals we also synthesized the new complex $[(\text{C}_5\text{Me}_4\text{PMe}_2\text{NAd})\text{Yb}(\text{CH}_2\text{SiMe}_3)_2]$ (7). Similar to 7_{Ad} the related complex 7 reveals a ^{31}P NMR signal at $\delta = -133.1$ ppm. Integration of

corresponding ^1H NMR signals of 7_{Ad} and 7 of the same paramagnetic shift region allowed the assignment of all signals. Both spectra show an almost mirror inverted order of shifts compared to all other paramagnetic complexes $[(\text{Cp}^{\text{TM}}\text{PN})\text{M}(\text{CH}_2\text{SiMe}_3)_2]$ ($\text{M} = \text{Sm}$ (4_{Ad}), Nd (5_{Ad}), Pr (6_{Ad})) or with $[(\text{C}_5\text{Me}_4\text{PMe}_2\text{NAd})\text{M}(\text{CH}_2\text{SiMe}_3)_2]$.¹⁷ In Fig. 3, the NMR spectrum of 7_{Ad} is shown as an example (for 7 see ESI†). The analogue praseodymium complex (6_{Ad}) displays a downfield shift of the diastereotopic protons $\text{Pr}-\text{CH}_2-\text{SiMe}_3$ to 93.03 and 99.51 ppm and an upfield shift of the adamantyl and annulated five-ring moiety protons to the range between -10 and -53 ppm (Fig. 2), whereas for 7_{Ad} both are shifted to the contrary way: the diastereotopic proton signals are shifted strongly upfield to -225.45 and -239.26 ppm and the adamantyl and annulated five-ring moiety signals are shifted strongly downfield to the range between 38 and 163 ppm. This trend can also be assigned for the other proton signals. It is a consequence of the sign variation of spin densities and therefore of the chemical shift within the lanthanide series.³¹

Molecular structures of $\text{Cp}^{\text{TM}}\text{PN}$ complexes

The molecular structures of $1_{\text{Ad}}-3_{\text{Ad}}$, 2_{Dip} and 3_{Dip} were established by X-ray structure analyses. Single crystals were obtained by cooling saturated *n*-hexane (2_{Dip} and 3_{Dip}) or *n*-pentane (1_{Ad}) solution to -30°C . One pentane molecule is incorporated in the unit cell of structure 1_{Ad} . Single crystals of 2_{Ad} were obtained from benzene at room temperature with one solvent molecule per unit cell. Single crystals of 3_{Ad} were obtained by slowly evaporating a toluene solution, while one toluene molecule is incorporated in the unit cell. Complexes $1_{\text{Ad}}-3_{\text{Ad}}$ crystallize in the triclinic space group $P\bar{1}$ with the two formal units in

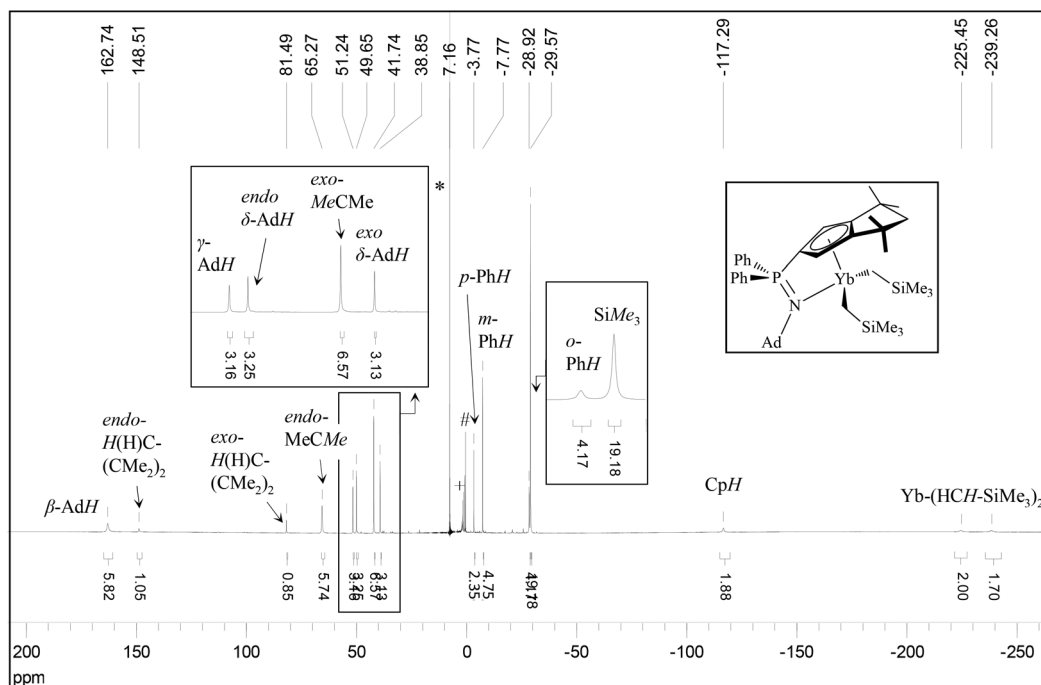


Fig. 3 ^1H NMR spectrum (500.2 MHz) of ytterbium complex **7Ad** in C_6D_6 at 27 $^\circ\text{C}$. Signals denoted with (*), (+) and (#) are assigned to SiMe_4 , silicon grease and the residual protons of C_6D_6 .

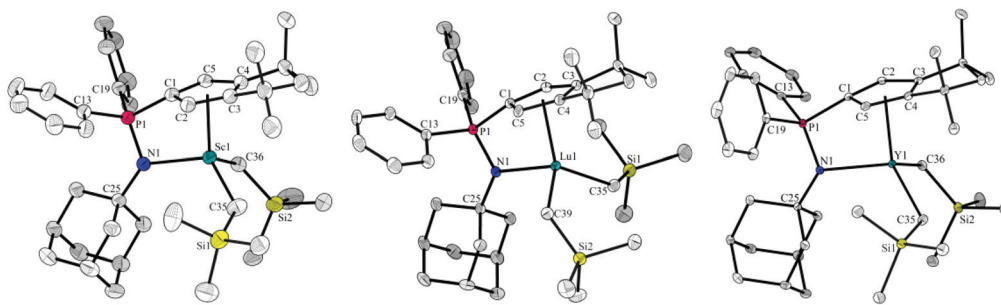


Fig. 4 Molecular structures of complexes $[\text{LAd}]\text{M}(\text{CH}_2\text{SiMe}_3)_2$ ($\text{Sc} = \mathbf{1Ad}$; $\text{Lu} = \mathbf{2Ad}$; $\text{Y} = \mathbf{3Ad}$). All hydrogen atoms and incorporated solvent molecules have been omitted for clarity.

the unit cell (Fig. 4). In contrast to **1Ad** the different incorporated solvent molecules in structures **2Ad** and **3Ad** have little effect on the unit cell and for that they are isostructural. Structures **2Dip** and **3Dip** are also isostructural and crystallize in the orthorhombic space group $Pbca$ with 8 formal units in the unit cell. Selected bond lengths (\AA) and angles ($^\circ$) for **1Ad**–**3Ad**, **2Dip** and **3Dip** are presented in Table 3. In the structure of the complexes **2Dip** and **3Dip** one of the CH_2SiMe_3 groups is disordered and treated with an occupancy factor of 56 : 44 and 62 : 38, respectively (Fig. 5).

Despite the sterically demanding Cp-moiety **1Ad**–**3Ad**, **2Dip** and **3Dip** reveal that the Cp ring coordinates to the metal centre in a typical η^5 mode, while IndPN adopt an η^3 -bonding fashion and the more bulky FluPN-type ligands have a rare η^1 -bonding mode.¹⁸ In the solid state, all complexes adopt mononuclear structures, in which the metal atoms reveal a *pseudo*-tetrahedral coordination by the η^5 -bonded C5-ring and

the nitrogen atom of the CpPN-ligand together with two σ -bonded alkyl groups. The *pseudo*-tetrahedral environment around the metal centre can be shown by comparison of the $\text{C}_{\text{CH}_2\text{SiMe}_3}\text{-M-N1}$, $\text{C}_{\text{CH}_2\text{SiMe}_3}\text{-M-N1}$, $\text{C}_{\text{CH}_2\text{SiMe}_3}\text{-M-C}_{\text{CH}_2\text{SiMe}_3}$ bond angles, which are all very close to 109° .

The average M–CH₂ bond lengths are comparable to those reported for $[\text{M}(\text{CH}_2\text{SiMe}_3)_3(\text{L})_x]$ complexes (for $\text{M} = \text{Sc}$;³³ Lu ;³⁴ Y).³⁵

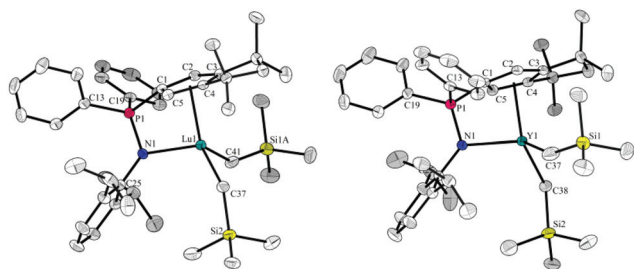
The P–C1 bond lengths in **1Ad**–**3Ad** (1.775(2), 1.775(2) and 1.776(2) \AA) are longer than in the free ligand (1.703(2) \AA), while the P–N bonds are essentially shorter (1.603(2), 1.596(2) and 1.605(2) \AA versus 1.653(2) \AA for **1Ad**). However, for **2Dip** and **3Dip** P–C1 bonds (1.767(4) and 1.758(4) \AA) are shorter (1.788(2) \AA) and P–N bonds (1.626(4) and 1.609(3) \AA) longer (1.556(2) \AA). The reason for this different behaviour is the different tautomeric forms of the free ligand.

The $\text{Cp}_{\text{centr.}}\text{-M-N}$ angles ($\text{M} = \mathbf{1Ad}$: 97.5; **2Ad**: 93.9; **3Ad**: 92.4; **2Dip**: 92.2; **3Dip**: 90.2 $^\circ$) are similar to those of $[\{\text{C}_5\text{Me}_4\text{PMe}_2\text{-}$



Table 3 Selected bond lengths (Å) and angles (°) for **1_{Ad}**, **2_{Ad}**, **3_{Ad}**, **2_{Dip}** and **3_{Dip}**

	1_{Ad}	2_{Ad}	3_{Ad}	2_{Dip}	3_{Dip}
P1–N1	1.603(2)	1.596(2)	1.605(2)	1.623(3)	1.610(3)
P1–C1	1.775(2)	1.775(2)	1.776(2)	1.767(4)	1.758(3)
M–N	2.210(2)	2.288(2)	2.339(2)	2.293(3)	2.342(3)
M–C _{CH₂SiMe₃}	2.236(2)	2.348(3)	2.407(2)	2.347(4)	2.40(2)
M–C _{CH₂SiMe₃}	2.215(2)	2.349(2)	2.409(2)	2.317(4)	2.400(3)
M–Z	2.288	2.371	2.419	2.409	2.455
C1–P1–N1	101.0(1)	102.4(1)	102.6(1)	100.7(2)	101.3(1)
Z–M–N1	97.5	93.9	92.4	92.2	90.2
C _{CH₂SiMe₃} –M–N1	115.7(1)	103.4(1)	103.4(1)	101.7(2)	100.2(6)
C _{CH₂SiMe₃} –M–N1	102.6(1)	112.8(1)	115.2(1)	115.4(1)	117.3(1)
C _{CH₂SiMe₃} –M–C _{CH₂SiMe₃}	104.1(1)	107.7(1)	108.6(1)	100.5(1)	100.5(6)
C1–P1–N1–C25	–172.2(2)	174.5(2)	–173.3(2)	155.5(3)	156.0(3)

**Fig. 5** Molecular structures of complexes $[(L_{\text{Dip}})M(\text{CH}_2\text{SiMe}_3)_2]$ ($\text{Lu} = 2_{\text{Dip}}$; $\text{Y} = 3_{\text{Dip}}$). All hydrogen atoms and disordered Me_3SiCH_2 -groups with lower occupancies have been omitted for clarity.

$\text{NAd}\}M(\text{CH}_2\text{SiMe}_3)_2]^{15,17}$ and are clearly smaller than the $\text{Cp}_{\text{centr.}}\text{--M--N}$ -angles in analogue $[(\eta^5\text{--}\eta^1\text{--CpSiN})M(\text{R})]$ CGC ($\text{M} = \text{Sc}$: 102.5;⁸ Lu : 98.3;³⁶ Y : 96.8°³³). Moreover, the real constrained geometry character of the complexes can be seen as they are significantly smaller than 109°.

In contrast to the long M–N bond found in $[(\text{C}_5\text{H}_4\text{PPh}_2\text{NDip})M(\text{CH}_2\text{SiMe}_3)_2(\text{thf})]$ the M–N bond lengths (**1_{Ad}**: 2.210(2); **2_{Ad}**: 2.288(2); **3_{Ad}**: 2.339(2); **2_{Dip}**: 2.293(4); **3_{Dip}**: 2.342(3) Å) are short and approach the length of an amide bond like in complexes $[(\text{C}_5\text{Me}_4\text{PMe}_2\text{NAd})M(\text{CH}_2\text{SiMe}_3)_2]^{15,17}$. They are closer to the covalent bonds represented by $[(\text{CpSiN})\text{--}M(\text{R})]$ ($\text{M} = \text{Sc}$: 2.083(5);^{7–9} Lu : 2.296(7);³³ Y : 2.327(5) Å)³³ and by $[M\{\text{N}(\text{SiMe}_3)_2\}_3]$ ($\text{M} = \text{Sc}$: av. 2.05;³⁷ Lu : av. 2.19;³⁸ Y : av. 2.22 Å)³⁹ than those in donor–acceptor complexes which can be demonstrated by an average value of $\text{M} = \text{Sc}$: 2.46 and Y : 2.60 Å⁴⁰ determined in $[(\text{Me}_3\text{TACN})M(\text{CH}_2\text{SiMe}_3)_3]$.

Conclusions

A new sterically most demanding CpPN chelate ligand system, cheaper than all tetramethyl-based building blocks and therefore more privileged to provide constrained-geometry complexes and catalysts of many more metals, has been developed. By condensation of NaCp with Ph_2PCl and with two molecules of acetone, followed by carbolithiation and Staudinger reaction of the phosphane $\text{Cp}^{\text{TM}}\text{HPPH}_2$ (**1**, diphenyl[4,4,6,6-tetramethyl-

1,4,5,6-tetrahydropentalen-2-yl)phosphane) with organic azides (AdN_3 and DipN_3 ; $\text{Ad} = 1\text{-adamantyl}$; $\text{Dip} = 2,6\text{-di-iso-propylphenyl}$), the two novel chelate ligands $\text{Cp}^{\text{TM}}\text{PPh}_2\text{NHAd}$ (**L_{Ad}H**) and $\text{Cp}^{\text{TM}}\text{HPPH}_2\text{NDip}$ (**L_{Dip}H**) were obtained in high selectivity and yields. Depending on the substituent at the nitrogen atom, they occur either in the *P*-amino-cyclopentadienylidene-phosphorane ($\text{R} = \text{Ad}$) or in the *P*-cyclopentadienyl-iminophosphorane ($\text{R} = \text{Dip}$) tautomeric form. Neither possesses any NMR detectable prototropic or elementotropic isomers. The rare-earth metal complexes were synthesized following a one-pot protocol, which combines deprotonation and salt elimination methods by addition of 3 equivalents of $\text{LiCH}_2\text{SiMe}_3$ as a base/ligand to a stirred mixture of the corresponding THF or DME solvated rare-earth metal trihalide and the appropriate $\{\text{Cp}^{\text{TM}}\text{PN}\}\text{H}$ ligand. The very short synthetic protocol allows the successful isolation of the highly reactive and labile alkyl complexes of early lanthanides, which are usually prone to decompose in solution at ambient temperature. All complexes $[(\text{Cp}^{\text{TM}}\text{PN})M(\text{CH}_2\text{SiMe}_3)_2]$ ($\text{M} = \text{Sc}$ (**1_{Ad}**, **1_{Dip}**), Lu (**2_{Ad}**, **2_{Dip}**), Y (**3_{Ad}**, **3_{Dip}**), Sm (**4_{Ad}**), Nd (**5_{Ad}**), Pr (**6_{Ad}**), Yb (**7_{Ad}**)) were isolated as microcrystalline solids and were completely characterized by microanalysis and partially by X-ray crystal structure determination. As a non-routine characterization method for organolanthanide complexes an extensive NMR study of a series of paramagnetic complexes with assignment of all signals is presented. Paramagnetic complexes Sm (**4_{Ad}**), Nd (**5_{Ad}**), Pr (**6_{Ad}**) reveal an almost mirror inverted signal order compared to previously unknown ytterbium(III) CpPN complexes **7_{Ad}** or its counterpart $[(\eta^1\text{--}\eta^5\text{--C}_5\text{Me}_4\text{PMe}_2\text{NAd})\text{Yb}(\text{CH}_2\text{SiMe}_3)_2]$ **7**.

Experimental section

General procedures

All manipulations were performed under purified argon or nitrogen using standard high vacuum or Schlenk- or Glovebox-techniques. Solvents were dried and distilled under argon employing standard drying agents. All organic reagents were purified by conventional methods. NMR spectra were recorded



at 300 K (27 °C) on a Bruker ARX200, Bruker AMX300, and Bruker AVANCE 500. Elemental analyses were performed at the Analytical Laboratory of the Chemistry Department/Philipps-Universität Marburg. EI mass spectra were taken on a Finnigan MAT CH7 spectrometer. The following starting materials were prepared according to the literature procedures: NaCp,²⁵ AdN₃,⁴¹ DipN₃,⁴² [Lu(CH₂SiMe₃)₃(thf)₂],⁴³ [ScCl₃(thf)₃],⁹ [MCl₃(dme)_n] (M = Lu, Y, Sm (*n* = 2); Nd, Pr, Ce (*n* = 1)),⁴⁴ LiCH₂SiMe₃⁴⁵ and C₅Me₄PMe₂NHAd.¹⁵

X-ray crystallographic studies

Suitable crystals were obtained from a concentrated benzene solution at room temperature (L_{Ad}H, 2_{Ad}), by cooling concentrated *n*-hexane (2_{Dip} and 3_{Dip}) or *n*-pentane (1_{Ad}) solution to −30 °C and by slow evaporation of toluene solution (3_{Ad}). Crystal data were collected with a Stoe-IPDS area-detector diffractometer using graphite-monochromatised Mo-K_α-radiation (λ = 71.073 pm) at 193 K (L_{Ad}H, 3_{Ad}, 2_{Dip}) or with a Stoe IPDS2 diffractometer at 100 K. Data reduction was carried out using the IPDSI software or X-Area (Stoe).⁴⁶ The data were empirically corrected for absorption and other effects by using multi-scans,⁴⁷ except for compound L_{Ad}H, where no improvement in the refinement was achieved through its application. The structures were solved by direct methods (Sir-92,⁴⁸ Sir-2004,⁴⁹ and SHELXS-97⁵⁰) and refined by full-matrix least-squares techniques against *F*_o² (SHELXL-97).⁴⁷ C bonded hydrogen atoms were included in idealized positions and refined with fixed isotropic displacement factors. The N-bonded hydrogen atom of L_{Ad}H was located and refined isotropically. The program PLATON⁵¹ was used to check the results of the X-ray analyses. Diamond was used for 30% thermal ellipsoid representations.⁵² CCDC no. 817338 (L_{Ad}H), 817339 (L_{Dip}H), 817340 (1_{Ad}), 817341 (2_{Ad}), 817342 (3_{Ad}), 817343 (2_{Dip}), and 817344 (3_{Dip}) contain the supplementary crystallographic data for this paper.

Synthesis of CpTMHPPH₂ (1). To 9.43 g Na(C₅H₅) (108 mmol, 1.03 eq.) in 200 mL of *n*-pentane at 0 °C, 23.16 mL of PPh₂Cl (105 mmol, 1.00 eq.) was added. The mixture was stirred for 16 h at ambient temperature, and then 10 mL of ethane-1,2-diol was added under vigorous stirring. The solution was decanted from the precipitate, the precipitate was washed twice with 20 mL of *n*-pentane, and the solvent of the transferred solution was evaporated in a vacuum. The following steps were carried out according to the literature, while spectroscopic features match perfectly with the reported ones.²⁴

Synthesis of ligand L_{Ad}H. To a solution of phosphane 1 CpTMHPPH₂ (2.40 g, 6.93 mmol, 1.00 eq.) in 30 mL of toluene, AdN₃ (1.35 g, 7.62 mmol, 1.10 eq.) was added and stirred at 120 °C for 17 h. The colour of the reaction mixture progressively turns brown. The reaction proceeding was monitored by ³¹P NMR spectroscopy. The solvent was completely removed in a vacuum and the oily residue was dissolved in 10 mL of *n*-hexane yielding a clear dark brown solution. Upon sonification of the *n*-hexane solution a yellow powder precipitated. It was filtered off, washed with 3 mL of *n*-hexane and dried in a vacuum. Yield: 2.33 g (4.70 mmol, 68%). M.p. =

176.5–177.0 °C. ¹H NMR (300.1 MHz, C₆D₆): δ = 1.44 (s, 6H, δ-AdH), 1.53 (s, 6H, β-AdH), 1.68 (s, 12H, CMe₂), 1.80 (br s, 3H, γ-AdH), 2.05 (d, ²J_{HP} = 5.0 Hz, 1H, NH), 2.46 (s, 2H, CH₂(CMe₂)₂), 6.17 (d, ³J_{HP} = 3.1 Hz, 2H, CpH), 7.00–7.03 (m, 6H, *m*-/*p*-PhH), 7.90–8.01 (m, 4H, *o*-PhH) ppm. ¹³C{¹H} NMR (75.5 MHz, C₆D₆): δ = 30.4 (s, γ-AdC), 33.4 (s, CMe₂), 36.2 (s, δ-AdC), 39.3 (d, ⁴J_{CP} = 1.3 Hz, CMe₂), 44.5 (d, ³J_{CP} = 4.0 Hz, β-AdC), 54.0 (d, ²J_{CP} = 2.0 Hz, α-AdC), 65.0 (s, CH₂(CMe₂)₂), 80.8 (d, ¹J_{CP} = 116.1 Hz, α-CpC), 106.6 (d, ²J_{CP} = 16.0 Hz, β-CpC), 128.5 (d, ³J_{CP} = 12.3 Hz, *m*-PhC), 131.7 (d, ⁴J_{CP} = 2.7 Hz, *p*-PhC), 131.9 (d, ¹J_{CP} = 105.3 Hz, *ipso*-PhC), 132.9 (d, ²J_{CP} = 10.5 Hz, *o*-PhC), 146.8 (d, ³J_{PC} = 18.5 Hz, γ-CpC) ppm. ³¹P{¹H} NMR (121.5 MHz, C₆D₆): δ = 15.6 (s) ppm. EI-MS: *m/z* (%) = 495 (70.1) [M⁺], 480 (100) [M⁺ – Me], 466 (5.2) [M⁺H – 2 Me], 135 (22.1) [Ad⁺]. Anal. calcd for C₃₄H₄₂PN (495.68): C 82.38, H 8.54, N 2.83; found C 81.40, H 8.45, N 2.59.

Synthesis of ligand L_{Dip}H. To a solution of CpTMHPPH₂ (6.59 g, 19.0 mmol, 1.00 eq.) in 75 mL of THF, DipN₃ (4.46 g, 21.9 mmol, 1.15 eq.) was added and stirred overnight at room temperature, whereupon N₂-evolution occurs. Removal of the solvent in a vacuum yielded a foamy residue. The compound was crystallized from acetonitrile at ambient temperature. A pale rose, crystalline solid was obtained. Yield: 7.51 g (14.4 mmol, 76%). M.p. = 142.5–143.0 °C. ¹H NMR (300.1 MHz, C₆D₆): δ = 1.00 (s, 6H, CMe₂), 1.03 (s, 6H, CMe₂), 1.18 (d, ³J_{HH} = 7.0 Hz, 12H, Me₂CH), 1.91 (s, 2H, CH₂(CMe₂)₂), 3.08 (s, 2H, CpCH₂), 3.66 (sept, ³J_{HH} = 6.8 Hz, 2H, Me₂CH), 6.77 (d, ³J_{HP} = 8.5 Hz, 1H, CpH), 7.03–7.06 (m, 6H, *m*-/*p*-PhH), 7.07–7.12 (m, 1H, *p*-DipH), 7.25 (d, ³J_{HH} = 7.4 Hz, 2H, *m*-DipH), 7.79–7.87 (m, 4H, *o*-PhH) ppm. ¹³C{¹H} NMR (75.5 MHz, C₆D₆): δ = 24.1 (s, Me₂CH), 29.1 (s, Me₂CH), 29.9 (s, CMe₂), 30.3 (s, CMe₂), 37.1 (d, ²J_{CP} = 10.4 Hz, β-CpCH₂), 40.0 (s, CMe₂), 41.8 (s, CMe₂), 61.6 (s, CH₂(CMe₂)₂), 119.9 (d, ⁵J_{CP} = 3.3 Hz, *p*-DipC), 123.2 (d, ⁴J_{CP} = 2.2 Hz, *m*-DipC), 128.6 (d, superimpose with residual protons of C₆D₆, *p*-PhC), 131.1 (d, ³J_{CP} = 2.5 Hz, *m*-PhC), 132.3 (d, ²J_{CP} = 9.6 Hz, *o*-PhC), 134.6 (d, ¹J_{CP} = 106.4 Hz, *ipso*-PhC), 140.7 (d, ²J_{CP} = 10.5 Hz, β-CpC), 142.6 (d, ¹J_{CP} = 100.0 Hz, α-CpC), 143.1 (d, ²J_{CP} = 6.9 Hz, *ipso*-DipC), 145.5 (s, *o*-DipC), 155.3 (d, ³J_{CP} = 14.5 Hz, γ-CpC), 163.2 (d, ³J_{CP} = 6.2 Hz, γ'-CpC) ppm. ³¹P{¹H} NMR (121.5 MHz, C₆D₆): δ = −15.8 (s) ppm. EI-MS *m/z* (%): 521 (47.0) [M⁺], 506 (31.6) [M⁺ – Me], 185 (56.2) [Ph₂P⁺]. Anal. calcd for C₃₆H₄₄NP (521.73): C 82.88, H 8.50, N 2.68; found C 82.53, H 8.57, N 2.88.

Synthesis of [(L_{Ad})Lu(CH₂SiMe₃)₂] (2_{Ad}). To a stirred solution of [Lu(CH₂SiMe₃)₂(thf)₂] (580 mg, 1.00 mmol, 1.00 eq.) in 10 mL of toluene, a solution of ligand L_{Ad}H (500 mg, 1.01 mmol, 1.01 eq.) in the same amount of solvent was added dropwise at ambient temperature. After 0.5 h the solvent was completely removed in a vacuum and the foamy residue was triturated with 10 mL of *n*-hexane, which results in dissolution and immediate deposition of a colourless crystalline solid. It was filtered off and dried in a vacuum. An additional amount of the compound can be obtained by storing the mother liquor at −30 °C. Yield: combined 660 mg (0.78 mmol, 78%). ¹H NMR (300.1 MHz, C₆D₆): δ = −0.58 (d, ²J_{HH} = 11.5 Hz, 2H, Lu-HCH), −0.19 (d, ²J_{HH} = 11.5 Hz, 2H, Lu-HCH), 0.48 (s, 18H,



SiMe₃), 1.19 (s, 6H, MeCMe), 1.45 (d, ²J_{HH} = 12.3 Hz, 3H, δ-AdH), 1.56 (d, ²J_{HH} = 12.4 Hz, 3H, δ-AdH), 1.64 (s, 6H, MeCMe), 1.92–1.97 (m, 3H, γ-AdH, superimpose with 1H, HCH(CMe₂)₂), 2.08 (s, 6H, β-AdH), 2.24 (d, ²J_{HH} = 13.1 Hz, 1H, HCH(CMe₂)₂), 5.96 (d, ³J_{HP} = 2.8 Hz, 2H, CpH), 6.99–7.08 (m, 6H, *p*-/*m*-PhH), 7.82–7.89 (m, 4H, *o*-PhH) ppm. ¹³C{¹H} NMR (62.9 MHz, C₆D₆): δ = 5.1 (s, SiMe₃), 30.5 (d, ⁴J_{CP} = 1.1 Hz, γ-AdC), 32.3 (s, MeCMe), 32.9 (s, MeCMe), 36.3 (s, δ-AdC), 40.1 (d, ⁴J_{CP} = 0.6 Hz, CMe₂), 40.6 (s, Lu-CH₂), 47.3 (d, ³J_{CP} = 8.4 Hz, β-AdC), 55.7 (d, ²J_{CP} = 7.2 Hz, α-AdC), 63.0 (s, CH₂(CMe₂)₂), 93.7 (d, ¹J_{CP} = 115.4 Hz, α-CpC), 106.7 (d, ²J_{CP} = 12.9 Hz, β-CpC), 128.6 (d, ⁴J_{CP} = 11.6 Hz, *p*-PhC), 131.2 (d, ¹J_{CP} = 87.0 Hz, *ipso*-PhC), 132.5 (d, ³J_{CP} = 2.9 Hz, *m*-PhC), 133.5 (d, ²J_{CP} = 10.6 Hz, *o*-PhC), 149.0 (d, ³J_{CP} = 13.9 Hz, γ-CpC) ppm. ³¹P{¹H} NMR (121.5 MHz, C₆D₆): δ = 6.4 (s) ppm. Anal. calcd for C₄₂H₆₃LuNPSi₂ (844.09): C 59.76, H 7.53, N 1.66; found: C 59.51, H 7.34, N 1.75.

Synthesis of [(L_{Dip})Lu(CH₂SiMe₃)₂] (2_{Dip}). 2_{Dip} was prepared using the same synthetic protocol as for 2_{Ad} starting from [Lu(CH₂SiMe₃)₃(thf)₂] (580 mg, 1.00 mmol, 1.00 eq.) and ligand L_{Dip}H (520 mg, 1.00 mmol, 1.00 eq.). The reaction was performed at 0 °C. A colourless, microcrystalline solid was obtained by storing the *n*-hexane solution at –30 °C in a yield of 480 mg (0.55 mmol, 55%). ¹H NMR (300.1 MHz, C₆D₆): δ = –0.56 (br s, 2H, Lu-HCH), –0.30 (br s, 2H, Lu-HCH), 0.37 (s, 18H, SiMe₃), 0.38 (d, 6H, Me₂CH superimpose with SiMe₃), 1.29 (s, 6H, MeCMe), 1.35 (br s, 6H, Me₂CH), 1.68 (s, 6H, MeCMe), 2.01 (d, ²J_{HH} = 13.0 Hz, 1H, HCH(CMe₂)₂), 2.36 (d, ²J_{HH} = 13.0 Hz, 1H, HCH(CMe₂)₂), 3.51 (sep, ³J_{HH} = 9.0 Hz, 2H, Me₂CH), 6.47 (d, ³J_{HP} = 2.6 Hz, 2H, CpH), 6.92–7.04 (m, 9H, *p*-/*m*-PhH, *p*-/*m*-DipH), 7.48–7.54 (m, 4H, *o*-PhH) ppm. ¹³C{¹H} NMR (62.9 MHz, C₆D₆): δ = 4.6 (s, SiMe₃), 22.7 (br s, Me₂CH), 24.1 (br s, Me₂CH), 29.0 (s, Me₂CH), 32.3 (s, MeCMe), 32.5 (s, MeCMe), 40.2 (s, CMe₂), 43.0 (s, Lu-CH₂), 62.6 (s, CH₂(CMe₂)₂), 93.3 (d, ¹J_{CP} = 113.3 Hz, α-CpC), 107.0 (d, ²J_{CP} = 12.8 Hz, β-CpC), 124.8 (d, ⁴J_{CP} = 3.6 Hz, *m*-DipC), 125.3 (d, ⁵J_{CP} = 3.7 Hz, *p*-DipC), 128.6 (d, ¹J_{CP} = 90.0 Hz, *ipso*-PhC), 128.8 (d, ⁴J_{CP} = 12.1 Hz, *p*-PhC), 132.7 (d, ³J_{CP} = 2.7 Hz, *m*-PhC), 132.9 (d, ²J_{CP} = 9.1 Hz, *o*-PhC), 133.4 (d, ²J_{CP} = 9.8 Hz, *ipso*-DipC), 145.7 (d, ³J_{CP} = 6.1 Hz, *o*-DipC), 150.1 (d, ³J_{CP} = 13.7 Hz, γ-CpC) ppm. ³¹P{¹H} NMR (121.5 MHz, C₆D₆): δ = 9.3 (s) ppm. Anal. calcd for C₄₄H₆₅LuNPSi₂ (870.13): C 68.27, H 7.53, N 1.61; found: C 67.76, H 7.39, N 1.80.

General procedure for the preparation of complexes

[{CpTMPPh₂NR}M(CH₂SiMe₃)₂] (M = Sc (R = Ad: 1_{Ad}; R = Dip: 1_{Dip}), Y (R = Ad: 3_{Ad}; R = Dip: 3_{Dip}), Sm (R = Ad: 4_{Ad}), Nd (R = Ad: 5_{Ad}), Pr (R = Ad: 6_{Ad}), Yb (R = Ad: 7_{Ad})) and [C₅Me₄PM₂NAd]Yb(CH₂SiMe₃)₂] 7

To a stirred suspension of [ScCl₃(thf)₃] or [MCl₃(dme)_x] (0.50 mmol, 1.00 eq.) and the protonated ligand (0.50 mmol, 1.00 eq.) in 15 mL of ether, a solution of LiCH₂SiMe₃ (1.50 mmol, 3.00 eq.) in 10 mL of toluene was added dropwise at 0 °C. The reaction mixture was stirred at 0 °C for another 0.5 h and concentrated in a vacuum to half of the original volume. LiCl was filtered off over Celite®. The solvent was

stripped off, whereupon a colourless foamy solid forms, which was crystallized from *n*-hexane. Storage at –30 °C followed by filtration and drying in a vacuum resulted in isolation of a microcrystalline solid.

Analytical data for [(L_{Ad})Sc(CH₂SiMe₃)₂] (1_{Ad}). Yield: 251 mg (0.35 mmol, 70%) of a colourless, microcrystalline solid. ¹H NMR (300.1 MHz, C₆D₆): δ = –0.08 (d, ²J_{HH} = 11.4 Hz, 2H, Sc-HCH), 0.46 (s, 18H, SiMe₃), 0.56 (d, ²J_{HH} = 11.4 Hz, 2H, Sc-HCH), 1.22 (s, 6H, MeCMe), 1.49 (d, ²J_{HH} = 12.3 Hz, 3H, δ-AdH), 1.60 (d, ²J_{HH} = 11.7 Hz, 3H, δ-AdH), 1.68 (s, 6H, MeCMe), 1.97–2.01 (m, 4H, γ-AdH superimpose with HCH(CMe₂)₂), 2.17 (d, ⁴J_{HP} = 2.0 Hz, 6H, β-AdH), 2.33 (d, ²J_{HH} = 13.0 Hz, 1H, HCH(CMe₂)₂), 5.94 (d, ³J_{HP} = 2.8 Hz, 2H, CpH), 7.00–7.07 (m, 6H, *m*-/*p*-PhH), 7.83–7.88 (m, 4H, *o*-PhH) ppm. ¹³C{¹H} NMR (75.5 MHz, C₆D₆): δ = 4.6 (s, SiMe₃), 30.7 (s, γ-AdC), 32.3 (s, MeCMe), 32.5 (s, MeCMe), 36.4 (s, δ-AdC), 40.4 (s, CMe₂), 40.4 (s, Sc-CH₂), 47.3 (d, ³J_{CP} = 8.3 Hz, β-AdC), 56.1 (d, ²J_{CP} = 7.1 Hz, α-AdC), 62.9 (s, CH₂(CMe₂)₂), 94.5 (d, ¹J_{CP} = 114.4 Hz, α-CpC), 107.1 (d, ²J_{CP} = 12.9 Hz, β-CpC), 128.5 (d, ⁴J_{CP} = 11.9 Hz, *p*-PhC), 130.9 (d, ¹J_{CP} = 86.9 Hz, *ipso*-PhC), 132.5 (d, ³J_{CP} = 2.8 Hz, *m*-PhC), 133.5 (d, ²J_{CP} = 10.5 Hz, *o*-PhC), 150.3 (d, ³J_{CP} = 13.7 Hz, γ-CpC) ppm. ³¹P{¹H} NMR (121.5 MHz, C₆D₆): δ = 7.3 (s) ppm. Anal. calcd for C₄₂H₆₃NPSi₂ (714.06): C: 70.65, H: 8.89, N: 1.96. Found: C: 67.79, H: 8.84, N: 2.03.

Analytical data for [(L_{Ad})Y(CH₂SiMe₃)₂] (3_{Ad}). Yield: 190 mg (0.25 mmol, 50%) of a colourless, microcrystalline solid. ¹H NMR (300.1 MHz, C₆D₆): δ = –0.39 (dd, ²J_{HH} = 11.2 Hz, ²J_{HY} = 2.7 Hz, 2H, Y-HCH), –0.04 (dd, ²J_{HH} = 11.2 Hz, ²J_{HY} = 2.7 Hz, 2H, Y-HCH), 0.47 (s, 18H, SiMe₃), 1.18 (s, 6H, MeCMe), 1.45 (d, ²J_{HH} = 12.0 Hz, 3H, δ-AdH), 1.56 (d, ²J_{HH} = 12.0 Hz, 3H, δ-AdH), 1.62 (s, 6H, MeCMe), 1.94 (s, 3H, γ-AdH), 1.96 (d, ²J_{HH} = 13.1 Hz, 1H, HCH(CMe₂)₂), 2.12 (s, 6H, β-AdH), 2.23 (d, ²J_{HH} = 13.1 Hz, 1H, HCH(CMe₂)₂), 6.05 (d, ³J_{HP} = 2.5 Hz, 2H, CpH), 7.05–7.21 (m, 6H, *p*-/*m*-PhH), 7.85–7.92 (m, 4H, *o*-PhH) ppm. ¹³C{¹H} NMR (75.5 MHz, C₆D₆): δ = 4.9 (s, SiMe₃), 30.5 (s, γ-AdC), 32.2 (s, MeCMe), 33.1 (s, MeCMe), 33.8 (d, ¹J_{CY} = 40.9 Hz, Y-CH₂), 36.3 (s, δ-AdC), 40.1 (s, CMe₂), 47.4 (d, ³J_{CP} = 8.7 Hz, β-AdC), 55.8 (d, ²J_{CP} = 6.9 Hz, α-AdC), 63.1 (s, CH₂(CMe₂)₂), 94.5 (d, ¹J_{CP} = 117.0 Hz, α-CpC), 106.8 (d, ²J_{CP} = 13.3 Hz, β-CpC), 128.6 (d, ⁴J_{CP} = 9.7 Hz, *p*-PhC), 131.4 (d, ¹J_{CP} = 86.5 Hz, *ipso*-PhC), 132.4 (d, ³J_{CP} = 2.8 Hz, *m*-PhC), 133.4 (d, ²J_{CP} = 10.6 Hz, *o*-PhC), 149.2 (d, ³J_{CP} = 13.8 Hz, γ-CpC) ppm. ³¹P{¹H} NMR (121.5 MHz, C₆D₆): δ = 6.5 (s) ppm. Anal. calcd for C₄₂H₆₃NPSi₂Y (758.01): C: 66.55, H: 8.38, N: 1.85. Found: C: 66.57, H: 7.98, N: 1.94.

Analytical data for [(L_{Ad})Sm(CH₂SiMe₃)₂] (4_{Ad}). Yield: 170 mg (0.21 mmol, 41%) of a yellow, microcrystalline solid. ¹H NMR (300.1 MHz, C₆D₆): δ = –7.18 (s, 6H, ν_{1/2} = 10 Hz, β-AdH), –4.80 (d, ²J_{HH} = 12.7 Hz, 1H, *endo*-HCH(CMe₂)₂), –2.15 (d, ²J_{HH} = 12.7 Hz, 1H, *exo*-HCH(CMe₂)₂), –1.58 (s, 6H, ν_{1/2} = 4 Hz, *endo*-MeCMe), –1.29 (s, 6H, ν_{1/2} = 3 Hz, *exo*-MeCMe), –1.12 (d, ²J_{HH} = 11.6 Hz, 3H, *endo*-δ-AdH), –0.73 (s, 3H, ν_{1/2} = 10 Hz, γ-AdH), –0.56 (d, ²J_{HH} = 11.6 Hz, 3H, *exo*-δ-AdH), 1.70 (s, 18H, ν_{1/2} = 2 Hz, SiMe₃), 7.74 (t, ³J_{HH} = 7.4 Hz, 2H, *p*-PhH), 7.94 (t, ³J_{HH} = 7.5 Hz, 4H, *m*-PhH), 10.34 (s, 4H, ν_{1/2} = 17 Hz,



o-PhH), 10.87 (s, 2H, $\nu_{1/2}$ = 9 Hz, CpH), 12.52 (br s, 2H, $\nu_{1/2}$ = 25 Hz, Sm-HCH), 12.65 (br s, 2H, $\nu_{1/2}$ = 22 Hz, Sm-HCH) ppm. $^{13}\text{C}\{^1\text{H}\}$ NMR (125.8 MHz, C_6D_6): δ = 4.3 (s, SiMe₃), 26.3 (s, MeCMe), 26.4 (s, γ -AdC), 28.5 (s, MeCMe), 32.1 (s, CMe₂), 33.2 (s, δ -AdC), 38.0 (s, β -AdC), 49.8 (s, α -AdC), 55.1 (s, CH₂(CMe₂)₂), 102.0 (s, β -CpC), 125.7 (s, γ -CpC), 129.6 (s, *m*-PhC), 133.4 (s, *p*-PhC), 135.7 (s, *o*-PhC) ppm. The signals of the Sm-CH₂, α -CpC and the *ipso*-PhC atoms could not be found in the ^{13}C -NMR-Spectrum. $^{31}\text{P}\{^1\text{H}\}$ NMR (121.5 MHz, C_6D_6): δ = 24.4 (br s) ppm. Anal. calcd for C₄₂H₆₃NPSi₂Sm (819.46): C: 61.56, H: 7.75, N: 1.71. Found: C: 60.61, H: 7.61, N: 2.02.

Analytical data for [(L_{Ad})Nd(CH₂SiMe₃)₂] (5_{Ad}). Yield: 164 mg (0.20 mmol, 40%) of a blue, microcrystalline solid. ^1H NMR (300.1 MHz, C_6D_6): δ = -27.26 (s, 6H, $\nu_{1/2}$ = 31 Hz, β -AdH), -24.05 (d, $^2J_{\text{HH}}$ = 10.2 Hz, 1H, *endo*-HCH(CMe₂)₂), -13.41 (s, 6H, $\nu_{1/2}$ = 16 Hz, *endo*-MeCMe), -12.29 (d, $^2J_{\text{HH}}$ = 8.5 Hz, 1H, *exo*-HCH(CMe₂)₂), -7.52 (d, $^2J_{\text{HH}}$ = 11.9 Hz, 3H, *endo*- δ -AdH), -6.47 (s, 3H, $\nu_{1/2}$ = 11 Hz, γ -AdH), -5.48 (s, 6H, $\nu_{1/2}$ = 8 Hz, *exo*-MeCMe), -4.93 (d, $^2J_{\text{HH}}$ = 10.2 Hz, 3H, *exo*- δ -AdH), 4.30 (s, 18H, $\nu_{1/2}$ = 10 Hz, SiMe₃), 9.13 (s, 2H, $\nu_{1/2}$ = 16 Hz, *p*-PhH), 9.92 (s, 4H, $\nu_{1/2}$ = 16 Hz, *m*-PhH), 12.03 (br s, 2H, $\nu_{1/2}$ = 58 Hz, CpH), 15.40 (s, 4H, $\nu_{1/2}$ = 23 Hz, *o*-PhH), 30.19 (br s, 2H, $\nu_{1/2}$ = 116 Hz, Nd-HCH), 33.48 (br s, 2H, $\nu_{1/2}$ = 132 Hz, Nd-HCH) ppm. $^{31}\text{P}\{^1\text{H}\}$ NMR (121.5 MHz, C_6D_6): δ = -92.0 (br s) ppm. Anal. calcd for C₄₂H₆₃NPSi₂Nd (813.34): C: 62.02, H: 7.81, N: 1.72. Found: C: 60.70, H: 7.86, N: 1.88.

Analytical data for [(L_{Ad})Pr(CH₂SiMe₃)₂] (6_{Ad}). Yield: 223 mg (0.28 mmol, 55%) of a light brown, microcrystalline solid. ^1H NMR (300.1 MHz, C_6D_6): δ = -52.96 (s, 6H, $\nu_{1/2}$ = 24 Hz, β -AdH), -45.27 (br d, 1H, $\nu_{1/2}$ = 26 Hz, *endo*-HCH(CMe₂)₂), -23.81 (d, $^2J_{\text{HH}}$ = 10.0 Hz, 1H, *exo*-HCH(CMe₂)₂), -21.50 (s, 6H, $\nu_{1/2}$ = 11 Hz, *endo*-MeCMe), -14.90 (d, $^2J_{\text{HH}}$ = 10.5 Hz, 3H, *endo*- δ -AdH), -14.21 (s, 3H, $\nu_{1/2}$ = 12 Hz, γ -AdH), -11.93 (s, 6H, $\nu_{1/2}$ = 7 Hz, *exo*-MeCMe), -10.72 (d, $^2J_{\text{HH}}$ = 10.5 Hz, 3H, *exo*- δ -AdH), 6.08 (s, 18H, $\nu_{1/2}$ = 6 Hz, SiMe₃), 10.65 (t, $^3J_{\text{HH}}$ = 6.8 Hz, 2H, *p*-PhH), 12.08 (t, $^3J_{\text{HH}}$ = 6.8 Hz, 4H, *m*-PhH), 20.73 (br s, 4H, $\nu_{1/2}$ = 24 Hz, *o*-PhH), 30.03 (s, 2H, $\nu_{1/2}$ = 26 Hz, CpH), 93.03 (br s, 2H, $\nu_{1/2}$ = 57 Hz, Pr-HCH), 99.51 (br s, 2H, $\nu_{1/2}$ = 60 Hz, Pr-HCH) ppm. $^{31}\text{P}\{^1\text{H}\}$ NMR (121.5 MHz, C_6D_6): δ = -66.0 (br s) ppm. Anal. calcd for C₄₂H₆₃NPSi₂Pr (810.01): C: 62.28, H: 7.84, N: 1.73. Found: C: 60.95, H: 7.89, N: 1.88.

Analytical data for [(L_{Ad})Yb(CH₂SiMe₃)₂] (7_{Ad}). Yield: 318 mg (0.38 mmol, 76%) of a dark red, microcrystalline solid. ^1H NMR (500.2 MHz, C_6D_6): δ = -239.26 (br s, 2H, $\nu_{1/2}$ = ca. 700 Hz, Yb-HCH), -225.45 (br s, 2H, $\nu_{1/2}$ = ca. 770 Hz, Yb-HCH), -117.29 (s, 2H, $\nu_{1/2}$ = ca. 309 Hz, CpH), -29.57 (s, 18H, $\nu_{1/2}$ = 40 Hz, SiMe₃), -28.92 (s, 4H, $\nu_{1/2}$ = 64 Hz, *o*-PhH), -7.77 (s, 4H, $\nu_{1/2}$ = 22 Hz, *m*-PhH), -3.77 (s, 2H, $\nu_{1/2}$ = 22 Hz, *p*-PhH), 38.85 (s, 3H, $\nu_{1/2}$ = 34 Hz, *exo*- δ -AdH), 41.74 (s, 6H, $\nu_{1/2}$ = 36 Hz, *exo*-MeCMe), 49.65 (s, 3H, $\nu_{1/2}$ = 34 Hz, *endo*- δ -AdH), 51.24 (s, 3H, $\nu_{1/2}$ = 48 Hz, γ -AdH), 65.27 (s, 6H, $\nu_{1/2}$ = 146 Hz, *endo*-MeCMe), 81.49 (s, 1H, $\nu_{1/2}$ = 49 Hz, *exo*-HCH(CMe₂)₂), 148.51 (s, 1H, $\nu_{1/2}$ = 178 Hz, *endo*-HCH(CMe₂)₂), 162.74 (s, 6H, $\nu_{1/2}$ = ca. 410 Hz, β -AdH) ppm. $^{31}\text{P}\{^1\text{H}\}$ NMR (202.5 MHz, C_6D_6): δ = -117.2 (br s) ppm. Anal. calcd for C₄₂H₆₃NPSi₂Yb (842.16): C: 59.90, H: 7.54, N: 1.66. Found: C: 58.94, H: 7.45, N: 1.71.

Analytical data for [(L_{Dip})Sc(CH₂SiMe₃)₂] (1_{Dip}). Yield: 132 mg (0.18 mmol, 36%) of a colourless solid. ^1H NMR (300.1 MHz, C_6D_6): δ = -0.07 (d, $^2J_{\text{HH}}$ = 11.3 Hz, 2H, Sc-HCH), 0.38 (s, 18H, SiMe₃), 0.40 (d, $^3J_{\text{HH}}$ = 6.6 Hz, 6H, MeCHMe), 0.50 (d, $^2J_{\text{HH}}$ = 11.3 Hz, 2H, Sc-HCH), 1.34 (s, 6H, MeCMe), 1.38 (d, $^3J_{\text{HH}}$ = 6.7 Hz, 6H, MeCHMe), 1.73 (s, 6H, MeCMe), 2.05 (d, $^2J_{\text{HH}}$ = 13.0 Hz, 1H, H(H)C(CMe₂)₂), 2.45 (d, $^2J_{\text{HH}}$ = 13.0 Hz, 1H, H(H)C(CMe₂)₂), 3.58 (sept, $^3J_{\text{HH}}$ = 6.7 Hz, 2H, MeCHMe), 6.52 (d, $^3J_{\text{HP}}$ = 2.4 Hz, 2H, HCp), 6.92–7.00 (m, 6H, *p*-*m*-PhH), 7.01–7.07 (m, 3H, *p*-*m*-DipH), 7.48–7.55 (m, 4H, *o*-PhH) ppm. $^{13}\text{C}\{^1\text{H}\}$ NMR (75.5 MHz, C_6D_6): δ = 4.1 (s, SiMe₃), 23.7 (br s, Me₂CH), 26.3 (br s, Me₂CH), 28.9 (s, Me₂CH), 31.9 (s, MeCMe), 32.6 (s, MeCMe), 40.4 (s, CMe₂), 45.2 (br s, Sc-CH₂), 62.6 (s, CH₂(CMe₂)₂), 94.2 (d, $^1J_{\text{CP}}$ = 112.6 Hz, α -CpC), 107.4 (d, $^2J_{\text{CP}}$ = 12.6 Hz, β -CpC), 124.9 (d, $^4J_{\text{CP}}$ = 3.5 Hz, *m*-DipC), 125.3 (d, $^5J_{\text{CP}}$ = 3.7 Hz, *p*-DipC), 128.5 (d, $^1J_{\text{CP}}$ = 82.6 Hz, *ipso*-PhC), 128.8 (d, $^4J_{\text{CP}}$ = 12.0 Hz, *p*-PhC), 132.7 (d, $^3J_{\text{CP}}$ = 2.8 Hz, *m*-PhC), 133.6 (d, $^2J_{\text{CP}}$ = 9.9 Hz, *o*-PhC), 140.9 (d, $^2J_{\text{CP}}$ = 9.9 Hz, *ipso*-DipC), 145.7 (d, $^3J_{\text{CP}}$ = 6.2 Hz, *o*-DipC), 151.0 (d, $^3J_{\text{CP}}$ = 13.5 Hz, γ -CpC) ppm. $^{31}\text{P}\{^1\text{H}\}$ NMR (121.5 MHz, C_6D_6): δ = 8.9 (s) ppm. Anal. calcd for C₄₄H₆₅NPScSi₂ (740.09): C: 71.41, H: 8.85, N: 1.89. Found: C: 70.33, H: 8.56, N: 2.07.

Analytical data for [(L_{Dip})Y(CH₂SiMe₃)₂] (3_{Dip}). Yield: 125 mg (0.16 mmol, 32%) of a colourless, microcrystalline solid. ^1H NMR (300.1 MHz, C_6D_6): δ = -0.31 (br d, $^2J_{\text{HH}}$ = 8.9 Hz, 2H, Y-HCH), -0.09 (br d, $^2J_{\text{HH}}$ = 9.0 Hz, 2H, Y-HCH), 0.39 (s, 18H, SiMe₃), 0.45 (s, 6H, MeCHMe), 1.29 (s, 6H, MeCMe), 1.35 (s, 6H, MeCHMe), 1.68 (s, 6H, MeCMe), 2.03 (d, $^2J_{\text{HH}}$ = 12.4 Hz, 1H, H(H)C(CMe₂)₂), 2.36 (d, $^2J_{\text{HH}}$ = 13.3 Hz, 1H, H(H)C(CMe₂)₂), 3.47 (sept, $^3J_{\text{HH}}$ = 6.8 Hz, 2H, MeCHMe), 6.49 (d, $^3J_{\text{HP}}$ = 2.6 Hz, 2H, CpH), 6.96–7.02 (br m, 9H, *p*-*m*-PhH, *p*-*m*-DipH), 7.50–7.57 (br m, 4H, *o*-PhH) ppm. $^{13}\text{C}\{^1\text{H}\}$ NMR (75.5 MHz, C_6D_6): δ = 4.4 (s, SiMe₃), 22.7 (br s, Me₂CH), 26.9 (br s, Me₂CH), 29.0 (s, Me₂CH), 31.9 (s, MeCMe), 32.2 (s, MeCMe), 37.1 (d, $^1J_{\text{CY}}$ = 42.3 Hz, Y-CH₂), 40.1 (s, CMe₂), 62.6 (s, CH₂(CMe₂)₂), 94.2 (d, $^1J_{\text{CP}}$ = 114.1 Hz, α -CpC), 107.0 (d, $^2J_{\text{CP}}$ = 12.9 Hz, β -CpC), 124.7 (d, $^4J_{\text{CP}}$ = 3.5 Hz, *m*-DipC), 125.1 (d, $^5J_{\text{CP}}$ = 3.9 Hz, *p*-DipC), 128.7 (d, $^4J_{\text{CP}}$ = 12.0 Hz, *p*-PhC), 130.8 (d, $^1J_{\text{CP}}$ = 97.5 Hz, *ipso*-PhC), 132.6 (d, $^3J_{\text{CP}}$ = 2.7 Hz, *m*-PhC), 133.3 (d, $^2J_{\text{CP}}$ = 9.8 Hz, *o*-PhC), 140.4 (d, $^2J_{\text{CP}}$ = 10.5 Hz, *ipso*-DipC), 145.4 (d, $^3J_{\text{CP}}$ = 6.0 Hz, *o*-DipC), 150.2 (d, $^3J_{\text{CP}}$ = 13.8 Hz, γ -CpC) ppm. $^{31}\text{P}\{^1\text{H}\}$ NMR (121.5 MHz, C_6D_6): δ = 9.1 (s) ppm.

Analytical data for [(C₅Me₄PM₂NAd)Yb(CH₂SiMe₃)₂] (7). Yield: 126 mg (0.19 mmol, 37%) of a dark red, microcrystalline solid. ^1H NMR (500.2 MHz, C_6D_6): δ = -243.89 (br s, 2H, $\nu_{1/2}$ = ca. 480 Hz, Yb-HCH), -215.83 (br s, 2H, $\nu_{1/2}$ = ca. 530 Hz, Yb-HCH), -71.44 (s, 6H, $\nu_{1/2}$ = 71 Hz, β -C₅Me₄), -38.71 (s, 6H, $\nu_{1/2}$ = 28 Hz, Me₂P), -18.37 (s, 18H, $\nu_{1/2}$ = 27 Hz, SiMe₃), 35.33 (s, 3H, $\nu_{1/2}$ = 32 Hz, *exo*- δ -AdH), 45.92 (s, 3H, $\nu_{1/2}$ = 26 Hz, *endo*- δ -AdH), 46.40 (s, 3H, $\nu_{1/2}$ = 42 Hz, γ -AdH), 104.27 (s, 6H, $\nu_{1/2}$ = 117 Hz, γ -C₅Me₄), 148.54 (s, 6H, $\nu_{1/2}$ = ca. 320 Hz, β -AdH) ppm. $^{31}\text{P}\{^1\text{H}\}$ NMR (121.5 MHz, C_6D_6): δ = -133.1 (br s) ppm. Anal. calcd for C₂₉H₅₅NPSi₂Yb (677.90): C: 51.38, H: 8.18, N: 2.07. Found: C: 50.06, H: 8.44, N: 2.12.



Acknowledgements

Financial support by DFG (Priority Program Lanthanide-Specific Functionality SPP-1166), by Chemetall GmbH, Frankfurt and by Studienstiftung des Deutschen Volkes is gratefully acknowledged. The authors thank Dr Thomas Linder for his contribution to the X-ray analysis of L_{AdH} .

Notes and references

- J. M. Birmingham and G. Wilkinson, *J. Am. Chem. Soc.*, 1956, **78**, 42–44; G. Wilkinson and J. M. Birmingham, *J. Am. Chem. Soc.*, 1954, **76**, 6210–6210.
- C. J. Schaverien, *Adv. Organomet. Chem.*, 1994, **36**, 283–362; H. Schumann, J. A. Meese-Marktscheffel and L. Esser, *Chem. Rev.*, 1995, **95**, 865–986; F. T. Edelmann, in *Comprehensive Organometallic Chemistry II*, ed. E. W. Abel, F. G. A. Stone and G. Wilkinson, Pergamon, Oxford, 1995, vol. 4, pp. 11–212.
- F. T. Edelmann, *Top. Curr. Chem.*, 1996, **179**, 247–276; H. Yasuda and E. Ihara, *Bull. Chem. Soc. Jpn.*, 1997, **70**, 1745–1767; Z. Hou and Y. Wakatsuki, *Coord. Chem. Rev.*, 2002, **231**, 1–22; G. A. Molander and J. A. C. Romero, *Chem. Rev.*, 2002, **102**, 2161–2185.
- S. Arndt and J. Okuda, *Chem. Rev.*, 2002, **102**, 1953–1976; Z. Hou, *Bull. Chem. Soc. Jpn.*, 2003, **76**, 2253–2266; V. C. Gibson and S. K. Spitzmesser, *Chem. Rev.*, 2003, **103**, 283–315; A.-S. Rodrigues and J.-F. Carpentier, *Coord. Chem. Rev.*, 2008, **252**, 2137–2154; M. Nishiura and Z. Hou, *Nat. Chem.*, 2010, **2**, 257–268.
- M. Z. Zimmermann and R. Anwender, *Chem. Rev.*, 2010, **110**, 6194–6259; P. Dröse, S. Blaurock, C. G. Hrib, L. Hilfert and F. T. Edelmann, *Z. Anorg. Allg. Chem.*, 2011, **637**, 186–189.
- H. Braunschweig and F. M. Breitling, *Coord. Chem. Rev.*, 2006, **250**, 2691–2720; J. Cano and K. Kunz, *J. Organomet. Chem.*, 2007, **692**, 4411–4423.
- P. J. Shapiro, W. D. Cotter, W. P. Schaefer, J. A. Labinger and J. E. Bercaw, *J. Am. Chem. Soc.*, 1994, **116**, 4623–4640.
- P. J. Shapiro, E. E. Bunel, W. P. Schaefer and J. E. Bercaw, *Organometallics*, 1990, **9**, 867–869.
- W. E. Piers, P. J. Shapiro, E. E. Bunel and J. E. Bercaw, *Synlett*, 1990, 74–84.
- J. Okuda, *Chem. Ber.*, 1990, **123**, 1649–1651.
- O. Tardif, Z. Hou, M. Nishiura, T.-A. Koizumi and Y. Wakatsuki, *Organometallics*, 2001, **20**, 4565–4573; O. Tardif, M. Nishiura and Z. Hou, *Tetrahedron*, 2003, **59**, 10525–10539.
- E. Ihara, M. Tanaka, H. Yasuda, N. Kanehisa, T. Maruo and Y. Kai, *J. Organomet. Chem.*, 2000, **613**, 26–32; Y. Takenaka and Z. Hou, *Organometallics*, 2009, **28**, 5196–5203.
- N. S. Hillesheim and J. Sundermeyer, *Terrae Rarae*, 2009, **17**, 1–5; N. S. Hillesheim, M. Elfferding, T. Linder and J. Sundermeyer, *Z. Anorg. Allg. Chem.*, 2010, **636**, 1776–1782.
- T. K. Panda, C. G. Hrib, P. G. Jones, J. Jenter, P. W. Roesky and M. Tamm, *Eur. J. Inorg. Chem.*, 2008, 4270–4279.
- K. A. Rufanov, A. R. Petrov, V. V. Kotov, F. Laquai and J. Sundermeyer, *Eur. J. Inorg. Chem.*, 2005, 3805–3807.
- A. R. Petrov, K. A. Rufanov, N. K. Hangaly, M. Elfferding, K. Harms and J. Sundermeyer, *Mendeleev Commun.*, 2010, **20**, 197–199.
- N. K. Hangaly, A. R. Petrov, K. A. Rufanov, K. Harms, M. Elfferding and J. Sundermeyer, *Organometallics*, 2011, **30**, 4544–4554.
- Z. Jian, A. R. Petrov, N. K. Hangaly, S. Li, W. Rong, Z. Mou, K. A. Rufanov, K. Harms, J. Sundermeyer and D. Cui, *Organometallics*, 2012, **31**, 4267–4282.
- Z. Jian, N. K. Hangaly, W. Rong, Z. Mou, D. Liu, S. Li, A. A. Trifonov, J. Sundermeyer and D. Cui, *Organometallics*, 2012, **31**, 4579–4587; Z. Jian, W. Rong, Z. Mou, Y. Pan, H. Xie and D. Cui, *Chem. Commun.*, 2012, **48**, 7516–7518.
- A. R. Petrov, K. A. Rufanov, B. Ziemer, P. Neubauer, V. V. Kotov and J. Sundermeyer, *Dalton Trans.*, 2008, 909–915.
- J. Sundermeyer, K. A. Rufanov, A. R. Petrov, M. Elfferding and M. Winkenstette, 2007, DE102007057854, EP2227479, US2011034715, WO2009068000.
- C. Freund, N. Barros, H. Gronitzka, B. Martin-Vaca, L. Maron and D. Bourissou, *Organometallics*, 2006, **25**, 4927–4930.
- P. Oulié, C. Freund, N. Saffon, B. Martin-Vaca, L. Maron and D. Bourissou, *Organometallics*, 2007, **25**, 6793–6804.
- A. R. Petrov, M. Elfferding, J. Möbus, K. Harms, K. A. Rufanov and J. Sundermeyer, *Eur. J. Inorg. Chem.*, 2010, 4157–4165.
- T. K. Panda, M. T. Gamer and P. W. Roesky, *Organometallics*, 2003, **22**, 877–878.
- H. L. Ammon, G. L. Wheeler and P. H. Watts, *J. Am. Chem. Soc.*, 1973, **95**, 6158–6163.
- C. Imrie, T. A. Modro, P. H. v. Rooyen, C. C. P. Wagener, K. Wallace, H. R. Hudson, M. McPartlin, J. B. Nasirun and L. Powroznik, *J. Phys. Org. Chem.*, 1995, **8**, 41–46.
- K. T. K. Chan, L. P. Spencer, J. D. Masuda, J. S. J. McCahill, P. Wei and D. W. Stephan, *Organometallics*, 2003, **23**, 381–390.
- M. P. Thornberry, C. Slebodnick, P. A. Deck and F. R. Fronczek, *Organometallics*, 2000, **19**, 5352–5369.
- K. C. Hultsch, P. Voth, T. P. Spaniol and J. Okuda, *Organometallics*, 2000, **19**, 228–243.
- I. Bertini and C. Luchinat, *Coord. Chem. Rev.*, 1996, **150**, 29–75; I. Bertini, C. Luchinat and G. Parigi, *Current Methods in Inorganic Chemistry; Volume 2, Solution NMR of Paramagnetic Molecules: Applications to Metallobiomolecules and Models*, Elsevier Science B.V., Amsterdam, 2001; G. N. La Mar, W. D. Horrocks Jr. and R. H. Holm, *NMR of Paramagnetic Molecules, Principles and Applications*, Academic Press, New York and London, 1973; H. Günther, *NMR-Spektroskopie – Grundlage, Konzepte und Anwendungen der Protonen und Kohlenstoff-13-Kernresonanz-Spektroskopie in der Chemie*, Thieme-Verlag, Stuttgart, 3rd edn, 1992.



- 32 A. Steudel, E. Siebel, R. D. Fischer, G. Paolucci and V. Lucchini, *J. Organomet. Chem.*, 1998, **556**, 229–238;
- L. Brachais and M. Visseaux, *Eur. J. Inorg. Chem.*, 2005, 2486–2492;
- J. Zou, D. J. Berg, D. Stuart, R. McDonald and B. Twamley, *Organometallics*, 2011, **30**, 4958–4967;
- M. V. R. Stainer and J. Takats, *J. Am. Chem. Soc.*, 1983, **105**, 410–415.
- 33 B. R. Elvidge, S. Arndt, P. M. Zeimentz, T. P. Spaniol and J. Okuda, *Inorg. Chem.*, 2005, **44**, 6777–6788.
- 34 H. Schumann, D. M. M. Freckmann and S. Decher, *Z. Anorg. Allg. Chem.*, 2002, **628**, 2422–2426.
- 35 S. Arndt, P. M. Zeimentz, T. P. Spaniol, J. Okuda, M. Honda and K. Tatsumi, *Dalton Trans.*, 2003, 3622–3627.
- 36 W.-X. Zhang, M. Nishiura and Z. Hou, *Chem.–Eur. J.*, 2007, **13**, 4037–4051.
- 37 J. S. Ghotra, M. B. Hursthouse and A. J. Welch, *J. Chem. Soc., Chem. Commun.*, 1973, 669–670.
- 38 G. Scarel, C. Wiemer, M. Fanciulli, I. L. Fedushkin, G. K. Fukin, G. A. Domrachev, Y. Lebedinskii, A. Zenkevich and G. Pavia, *Z. Anorg. Allg. Chem.*, 2007, **633**, 2097–2103.
- 39 M. Westerhausen, M. Hartmann, A. Pfitzner and W. Schwarz, *Z. Anorg. Allg. Chem.*, 1995, **621**, 837–850.
- 40 C. S. Tredget, S. C. Lawrence, B. D. Ward, R. G. Howe, A. R. Cowley and P. Mountford, *Organometallics*, 2005, **24**, 3136–3148;
- S. Bambirra, A. Meetsma and B. Hessen, *Acta Crystallogr., Sect. E: Struct. Rep. Online*, 2006, **62**, m314–m317.
- 41 G. K. S. Prakash, M. A. Stephenson, J. G. Shih and G. A. Olah, *J. Org. Chem.*, 1986, **51**, 3215–3217.
- 42 L. P. Spencer, R. Altwer, P. Wei, L. Gelmini, J. Gault and D. W. Stephan, *Organometallics*, 2003, **22**, 3841–3854.
- 43 H. Schumann and J. Müller, *J. Organomet. Chem.*, 1979, **169**, C1–C4.
- 44 D. B. Dell'Amico, F. Calderazzo, C. D. Porta, A. Merigo, P. Biagini, G. Lugli and T. Wagner, *Inorg. Chim. Acta*, 1995, **240**, 1–3;
- U. Baisch, D. B. Dell'Amico, F. Calderazzo, R. Conti, L. Labella, F. Marchetti and E. A. Quadrelli, *Inorg. Chim. Acta*, 2004, **357**, 1538–1548.
- 45 G. D. Vaughn, K. A. Krein and J. A. Gladysz, *Organometallics*, 1986, **5**, 936–942.
- 46 Stoe & Cie GmbH: *IPDS Software*, Darmstadt, Germany, 1996; *X-Area and X-RED32*, Darmstadt, Germany, 2006.
- 47 R. H. Blessing, *Acta Crystallogr., Sect. A: Fundam. Crystallogr.*, 1995, **A51**, 33–38.
- 48 G. Cascarano, L. Favia and C. Giacovazzo, *J. Appl. Crystallogr.*, 1992, **25**, 310–317.
- 49 M. C. Burla, R. Caliandro, M. Camalli, B. Carrozzini, G. L. Cascarano, L. De Caro, C. Giacovazzo, G. Polidori and R. Spagna, *J. Appl. Crystallogr.*, 2005, **38**, 381–388.
- 50 G. M. Sheldrick, *Acta Crystallogr., Sect. A: Fundam. Crystallogr.*, 2008, **A64**, 112–122.
- 51 A. L. Spek, *Acta Crystallogr., Sect. A: Fundam. Crystallogr.*, 1990, **46**, C34.
- 52 K. Brandenburg, *Diamond, Release 3.0, Crystal Impact GbR*, Bonn, Germany, 2004.

